

Article

Quantitative and Qualitative Experimental Assessment of Water Vapor Condensation in Atmospheric Air Transonic Flows in Convergent–Divergent Nozzles

Mirosław Majkut ¹, Sławomir Dykas ^{1,*}, Krystian Smolka ^{1,*}, Tim Wittmann ², Axel Kuhlmann ²
and Florian Thorey ³

¹ Department of Power Engineering and Turbomachinery, Silesian University of Technology, 44-100 Gliwice, Poland; miroslaw.majkut@polsl.pl

² Center of Computational Energy, Airbus Operations GmbH, Kreetzlag 10, 21129 Hamburg, Germany

³ Airbus Operations SAS, 316 Route de Bayonne, 31060 Toulouse, France

* Correspondence: slawomir.dykas@polsl.pl (S.D.); krystian.smolka@polsl.pl (K.S.)

Abstract: Atmospheric air, being also a moist gas, is present as a working medium in various areas of technology, including the areas of airframe aerodynamics and turbomachinery. Issues related to the condensation of water vapor contained in atmospheric air have been intensively studied analytically, experimentally and numerically since the 1950s. An effort is made in this paper to present new, unique and complementary results of the experimental testing of moist air expansion in the de Laval nozzle. The results of the measurements, apart from the static pressure distribution on the nozzle wall and the images obtained using the Schlieren technique, additionally contain information regarding the quantity and quality of the condensate formed due to spontaneous condensation at the transition from the subsonic to the supersonic flow in the nozzle. The liquid phase was identified using the light extinction method (LEM). The experiments were performed for three geometries of convergent–divergent nozzles with different expansion rates of 3000, 2500 and 2000 s^{−1}. It is shown that as the expansion rate increases, the phenomenon of water vapor spontaneous condensation appears closer to the critical cross-section of the nozzle. A study was performed of the impact of the air relative humidity and pollution on the process of condensation of the water vapor contained in the air. As indicated by the results, both these parameters have a significant effect on the flow field and the pressure distribution in the nozzle. The results of the experimental analyses show that in the case of the atmospheric air flow, in addition to the pressure, temperature and velocity, other parameters must also be taken into account as boundary parameters for possible numerical analyses. Omitting information about the air humidity and pollution can lead to incorrect results in numerical simulations of transonic flows of atmospheric air. The presented results of the measurements of the moist air transonic flow field are original and fill the research gap in the field of experimental studies on the phenomenon of water vapor spontaneous condensation.

Keywords: experimental tests; moist air; de Laval nozzle; condensation; two-phase flow



Citation: Majkut, M.; Dykas, S.; Smolka, K.; Wittmann, T.; Kuhlmann, A.; Thorey, F. Quantitative and Qualitative Experimental Assessment of Water Vapor Condensation in Atmospheric Air Transonic Flows in Convergent–Divergent Nozzles. *Energies* **2024**, *17*, 5459. <https://doi.org/10.3390/en17215459>

Academic Editors: Marco Marengo and Magdalena Piasecka

Received: 5 September 2024

Revised: 15 October 2024

Accepted: 28 October 2024

Published: 31 October 2024



Copyright: © 2024 by the authors. Licensee MDPI, Basel, Switzerland. This article is an open access article distributed under the terms and conditions of the Creative Commons Attribution (CC BY) license (<https://creativecommons.org/licenses/by/4.0/>).

1. Introduction

Air and water are two substances that are necessary for human life. They have also been widely used in technology as carriers of energy (potential, kinetic or thermal) for hundreds, if not thousands, of years. Of course, this does not mean that everything is already known and obvious when it comes to the physical phenomena involving air or water. Atmospheric air is humid—it is a mixture of dry air and water in the gaseous (water vapor), liquid (water droplets) or solid (ice crystals) phase. However, the most common form of H₂O in air is water vapor. The most popular measure of the presence of water vapor in the air is the relative humidity, which is the ratio of the amount of water vapor contained in the air to the amount of water vapor the air can hold at a given temperature

and pressure. As moist air heats up, its relative humidity decreases, while cooling leads to an increase in its relative humidity, although in both cases the actual mass fraction of water vapor in the air remains the same. Rapid cooling of air can involve rapid condensation of the water vapor contained in it. The faster the cooling, the more violent the condensation process. The research issues related to water vapor condensation in transonic flows of moist (atmospheric) air have been the focus of interest for years now. It is an important research area as it concerns a number of flow issues related to the aerodynamics of aircraft (airplanes or missiles) and problems related to turbomachinery, fans, or compressors of turbine aircraft engines. Moreover, the array of issues where these phenomena occur is extremely wide, ranging from pneumatic systems to gas separation devices.

The literature survey suggests that the research issues need systematizing and dividing into problems related to analytical, experimental and numerical testing. There are, of course, works that combine all these aspects, but due to publication-related limitations, they fail to provide a great deal of important information, which makes most of them projects of a rather survey-type nature.

The genesis of the research on condensation in moist air dates back to the mid-1930s, when at the 1935 Volta meeting Prandtl presented a Schlieren image showing two oblique pressure waves crossing each other near the throat of a nozzle without backpressure [1]. Wieselberger, participating in the meeting, noted that the structure depended on the initial value of the air relative humidity. In the years 1934–1936, Hermann published some results on these perturbations, calling them “condensation waves” and noting that near the throat they were perpendicular (high humidity), while further downstream they took on an X-shaped structure (low humidity) [2]. In 1942, Oswatitsch presented a general kinetic and thermodynamic theory for describing condensation in convergent–divergent nozzles [3]. Since then, research on condensation has been carried out continuously until today. Prof. Jürgen Zierep, a disciple of Oswatitsch and indirectly of Prandtl, initiated research at the University of Karlsruhe, where he held the Chair of Fluid Mechanics in 1961. The research involved both theoretical analyses [4] and, above all, experimental studies [5,6]. Schnerr’s early works [6,7], which provided very valuable data for the validation of many numerical methods and models, are especially noteworthy in the area of experimental studies.

The first studies on the numerical methods used for modeling the condensation phenomenon date back to the 1960s. Most often, they concerned the notation and methods of solving one-dimensional conservation equations with the steady-state condensation model in the de Laval nozzle. However, they usually concerned pure water vapor and not moist air [8–10]. A systematic and uniform theory of the effect of aerodynamic waves and condensation waves for a mixture of air and water vapor was presented by Guha [11]. In the area of rather scarce experimental studies on transonic condensing moist air flows, in addition to Schnerr’s works, the results presented by other researchers also deserve mentioning, including the experimental studies performed for the half nozzle [12] or for the symmetric and asymmetric nozzle [13,14].

In the area of CFD studies on transonic flows of condensing moist air, growing interest has been observed since the early 1990s. The works were initiated by Schnerr’s research team, which contributed significantly to the development of condensation models used to model the transonic flow of moist air [15–18]. The numerical studies include the search for new CFD methods intended for modeling such flows. They typically center on the RANS methods for different descriptions of the two-phase flow, either to write conservation equations for the air/vapor mixture [19,20], or for the two phases separately using Euler–Euler [21] or Euler–Lagrange [22] methods. Another trend in the numerical research in this area aims to improve the condensation model itself, i.e., to offer a better description of the process of nucleation and droplet growth [23]. The developed numerical models have been used to analyze the flow phenomena that facilitate the interpretation of physical phenomena and the design of many engineering applications, such as ejectors, separators or compressors. Marynowski et al. focused on finding an optimal CFD method to model moist air condensing flows through ejectors [24] while, for example, Zhang G. et al. studied

the impact of relative air humidity and pollution on the process of vapor condensation in ejectors [19,25].

While it is possible to find new publications presenting numerical studies on the process of non-equilibrium condensation of water vapor in transonic flows of atmospheric air, there is a considerable lack of experimental research in this field. In the vast majority, the current works involving experimental studies on the measurement of the parameter of the condensing flow of water vapor contained in atmospheric air concern equilibrium condensation, related to the slow cooling of atmospheric air in recuperators, i.e., air flows occurring at a much lower speed. They mainly focus on studies of the process of equilibrium condensation and heat exchange, and on the two-phase structures arising in flows through channels [26,27]. Siddiqui M. et al. conducted a very interesting experimental and numerical study related to the parametric evaluation of the amount of water condensing in a plain heat exchanger [28].

However, in order to validate the CFD methods and computational models developed for the condensing moist air flow, new experimental studies are required to include information on the liquid phase, in addition to flow field visualization by means of the Schlieren technique and the static pressure measurement.

This paper presents the results of experimental studies that are a continuation of previous research in the area of analysis of the condensation phenomenon in transonic flows of moist air [13,14]. The research technique was expanded to include the light extinction method (LEM), which enables a quantitative assessment of the liquid phase arising due to water vapor condensation [29]. Information on the flow field, as well as on the dispersed liquid phase raised by non-equilibrium condensation, is most often experimental data for transonic flows of moist air. In contrast, for condensing moist air flow at a much lower velocity, it is possible to determine the heat transfer characteristics of the steam condensation flow [30].

2. Experimental Facility

The experiments presented herein were carried out on the air system available at the Department of Power Engineering and Turbomachinery of the Silesian University of Technology. It consists of a screw compressor, a Roots blower, a vacuum tank, a pressure tank and appropriate fittings in the form of pipelines and valves. The system can operate in an open- as well as in a closed-loop configuration (Figure 1). It is fitted with an automation system for remote operation and control.

2.1. Test Rig and Test Section

The wind tunnel test rig operating in an open-loop system (i.e., sucking ambient atmospheric air into the vacuum tank in the continuous mode, with the Roots blower on), due to the blower limitations, produces a constant pressure of about 52 kPa in the tank. This is also the pressure that usually prevails at the outlet of the tested nozzles during experiments performed in the test channel.

Another operating mode is pulsatory operation. In this mode, low initial pressure, in the order of 10 kPa, is produced in the vessel by means of a vane vacuum pump. As operation continues, the pressure increases. As the tank fills with air, a critical flow of ~ 0.1 kg/s lasting for about 20 s arises in the nozzle, with a backpressure of 10 to 60 kPa. Figure 2 shows the measuring channel used to measure the flows in symmetric de Laval nozzles. The width of the flow channel is 20 mm. The geometry of the nozzles in the channel can be interchanged. The flow channel was designed in this way to make it possible to place the nozzle geometry with taps for pressure measurements at a distance of every 5 mm, starting downstream of the critical section. In measurements, it is usually only the top half of the nozzle that has pressure-measuring taps, but this solution can also be used for the bottom half, for both halves, or not at all.

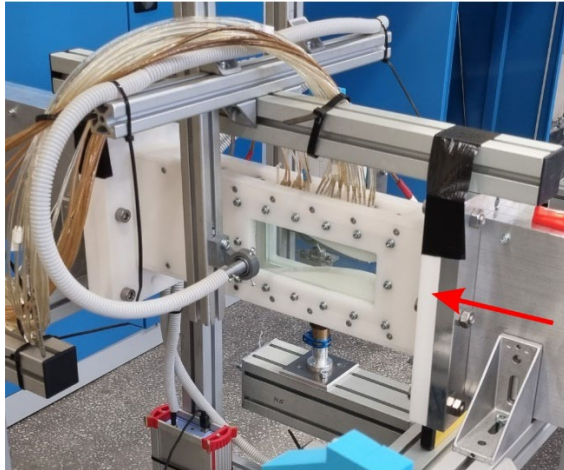
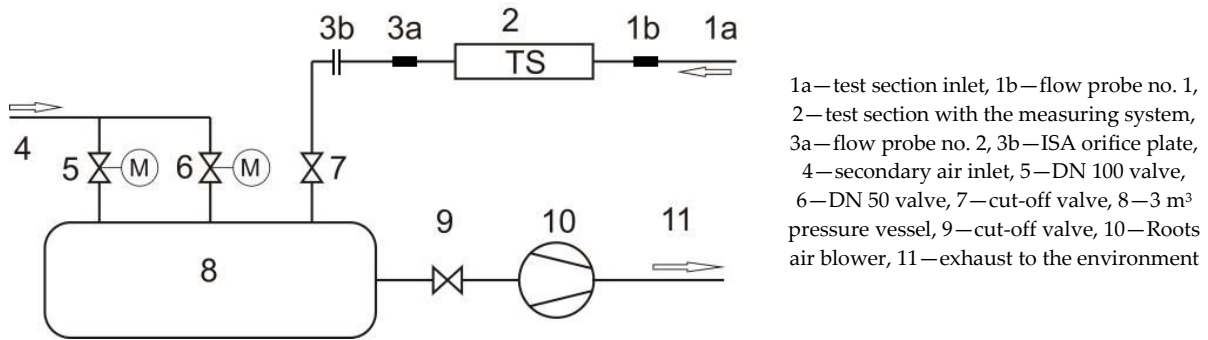


Figure 1. Elements of the wind tunnel test rig operating in a continuous mode.

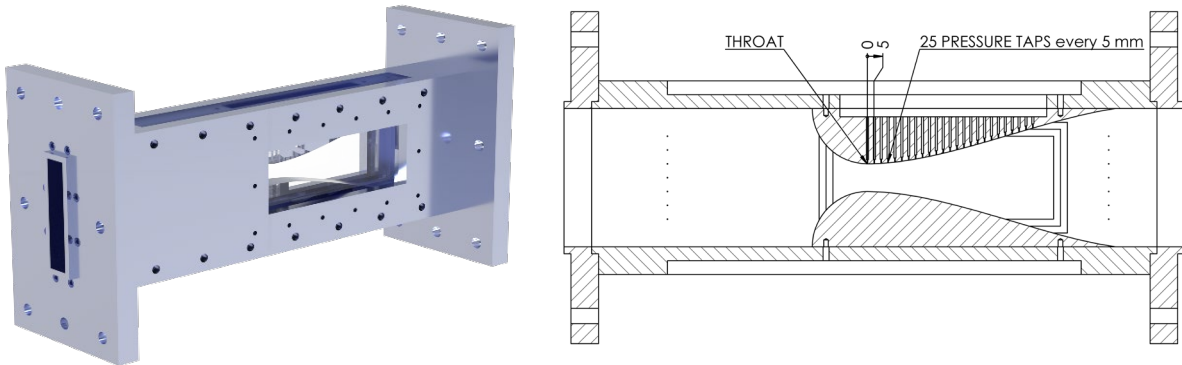


Figure 2. Test channel—diagram and design details.

The test section with nozzles was manufactured by CNC machining from a material called polyoxymethylene (POM), which is an engineering thermoplastic perfect for parts requiring high stiffness, low friction, and excellent dimensional stability.

2.2. Investigated Geometry

Three geometries of de Laval convergent–divergent nozzles were tested in this case. They were characterized by different expansion rates, as defined according to Formula (1).

$$\dot{p} = \frac{c_{0,inlet}}{p_{0,inlet}} \cdot \frac{p_{inlet} - p_{outlet}}{l} \tag{1}$$

Table 1 presents the velocity values of the tested nozzles, their geometry and the approximating polynomial coefficients. It should not be forgotten that in the case of critical flows through a nozzle, the shape of the de Laval convergent part has no effect on the

distributions of the parameters in the divergent, supersonic part. It is only important that the convergent to divergent part's curve profile transition be tangent, maintaining the continuity of the first derivative. Otherwise, instances of separation or oblique shock waves may occur.

Table 1. Data of the tested nozzles.

Nozzle Geometry		$y=b_0+b_1x+b_2x^2+b_3x^3+b_4x^4$
Nozzle 1 $\dot{p} \approx 3000 \frac{1}{s}$		$b_0 = 1.000 \times 10^{-2}$ $b_1 = 2.273 \times 10^{-3}$ $b_2 = 3.293$ $b_3 = -1.613 \times 10$ $b_4 = 2.989 \times 10$
Nozzle 2 $\dot{p} \approx 2500 \frac{1}{s}$		$b_0 = 1.000 \times 10^{-2}$ $b_1 = -1.346 \times 10^{-2}$ $b_2 = 1.239$ $b_3 = 3.215 \times 10^{-2}$ $b_4 = 1.965$
Nozzle 3 $\dot{p} \approx 2000 \frac{1}{s}$		$b_0 = 1.000 \times 10^{-2}$ $b_1 = -3.116 \times 10^{-3}$ $b_2 = 6.501 \times 10^{-1}$ $b_3 = -4.696 \times 10^{-1}$ $b_4 = 2.794$

2.3. Experimental Techniques

The inlet boundary conditions, i.e., ambient pressure, ambient temperature, relative humidity and airborne particulate content (PM1, PM2.5, PM4, PM10), were determined according to averaged measurements using an APAR AR258 transducer installed on the tunnel inlet pipeline. The transducer measuring ranges were as follows: PM : 1–1000 $\mu\text{g}/\text{m}^3$; p : 300–1100 hPa, Φ : 0–100%, t : -10 – $+60$ $^{\circ}\text{C}$.

For this transducer, the measurement of the mass of solid particles of a given diameter in the air volume is summed as the particle diameter increases from 1 to 10 μm , which means that the measurement for the largest particles is the sum of the measurements for all the particles with a smaller diameter. In other words, if the measurement value for PM1 and PM2.5 is the same, it means that particles with the diameter of 1 μm dominate. The static pressure on the nozzle's top wall was measured using 25 Aplisens PC-28 pressure transducers with the measuring range of 0–160 kPa of absolute pressure, with an accuracy of 0.1%. The pressure transducers used in the measuring system underwent additional calibration to increase their resolution to ± 100 Pa. This resolution was achieved through segment calibration, taking into account the hysteresis phenomenon of each transducer over their entire measuring range. Control air temperature measurements were also carried out, using a thermocouple placed at the inlet of the nozzle measuring section. The density gradients were visualized by means of a Schlieren set including parabolic mirrors and a high-speed Phantom Miro C110 camera in the "Z+" configuration developed at the SUT.

From the point of view of a correct estimation of the presence of water vapor in the air, a very important aspect is the information about the diameter and number of liquid-phase particles in the flowing medium. For this purpose, an optical method based on the light absorption technique was used in the presented research. As technology develops, these methods provide more and more accurate and reproducible results. Their most important advantages can be formulated as follows:

- Possibility of obtaining information on not only the water vapor wetness factor but also the size and concentration of liquid phase droplets.
- Measuring fiber-optic probes are treated as non-invasive (or hardly invasive) due to the transparency of the measuring space, where only light is present.
- Analysis of scattered light data is usually carried out for the visible and UV wavelength range (240–800 nm), so simple and relatively inexpensive optics and spectroscopy systems can be used.
- Sampling is unnecessary as measurements can be made directly inside the test space; local thermodynamic parameters are not disturbed.
- Measurement is fast, possibly within a few milliseconds depending on the size of the measuring space and used equipment.

The method for determining the size and number of droplets based on light scattering is often referred to as the light extinction method (LEM) or the turbidity method. We benefited from the experience and excellent knowledge in this field of Prof. Cai [31,32]. The light extinction method (LEM) was successfully implemented in our laboratories for measurements of the liquid phase of both in-steam and moist air flows [33]. In the LEM method, a wave with wavelength λ and reference intensity $I_0(\lambda)$, after passing distance L through a medium of homogeneous particles (droplets), is attenuated to intensity $I(\lambda)$ (Figure 3).

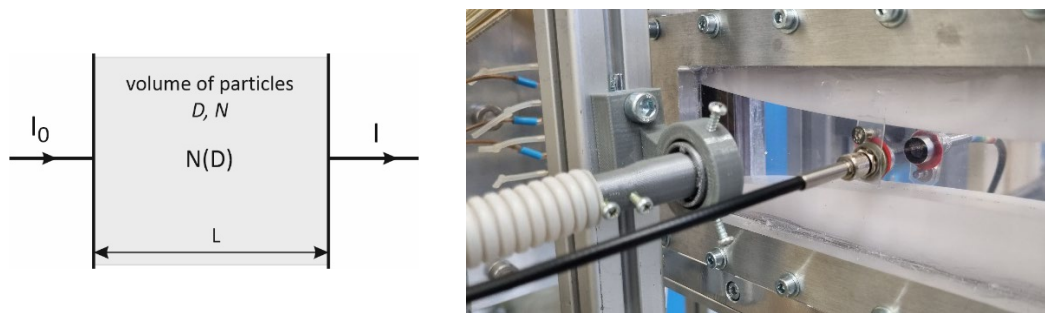


Figure 3. Attenuation of reference I_0 after crossing distance L in the light extinction method, and two types of LEM probes mounted in the test section.

In the first phase, the procedure consists of determining the relations resulting from the Bouguer–Lambert–Beer law for the entire measured range of the light wavelength. This principle is graphically presented in Figure 4, which shows a curve illustrating the dependence of the measured extinction coefficient on the wavelength.

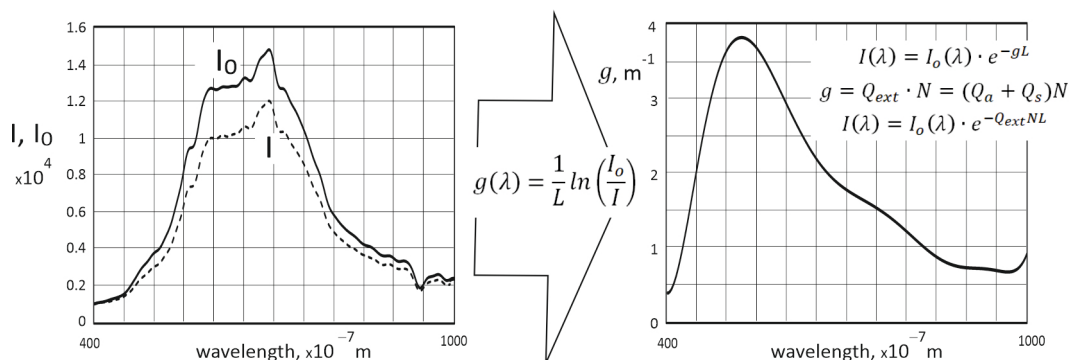


Figure 4. Light intensity curves I and I_0 (experimental measurement) and changes in the coefficient g as a function of the light wavelength.

The curve illustrating the light scattering by a particle depends mainly on the ratio between the refractive index for the particle and the environment (n) and on the ratio

between the particle perimeter (D) and the incident light wavelength (λ). These relations are considered in the quantity referred to as the Mie parameter:

$$X = \frac{\pi D}{\lambda}. \quad (2)$$

At very low values of parameter $X \ll 1$, the particle is very small compared to λ , the scattering field shape corresponds to a dipole, and the forward-scattered radiation (i.e., in the direction of incident light propagation) and backward-scattering radiation are practically identical. In such a case, the common method using a probe with mirrors is insufficient and its application is rather impossible. Starting from $X > 1$, the forward scattering becomes noticeably higher than the backward scattering. However, the concentration of droplets in a kilogram of air in the moist air flow under the measuring conditions is not too high (usually in the order of about 10^{12} – 10^{15} kg^{-1}) and the droplets are very small ($< 700 \text{ nm}$). For this reason, extinction is very difficult to measure in this situation. Moreover, the size of most of the droplets is within the limits of the Mie method's application range. Theoretically, the Mie parameter for the smallest particles recorded at the UV light's lowest applied wavelength (240 nm), with an acceptable extinction efficiency ($Q_{ext} > 0.5$), is $X > 1.75$, which, if converted to the minimum droplet size for the method, gives $D > 134 \text{ nm}$. The measurements under real conditions are also hampered by the need to determine intensity I_0 as accurately as possible, taking into account the small number of particles and thus the low turbidity of the medium in the measuring space. In the case of fluid flows with large temperature gradients, another problem can appear: the condensation phenomenon occurring on the surfaces of the tunnel windowpanes during the measurement of the reference intensity, i.e., usually in the absence of flow. Therefore, in order to determine I_0 , measurement under no-flow steady-state conditions for ideally dry air is recommended.

In a further step, using the relations presented in Figure 4 and derived from the Mie law, coefficient Q_{ext} and the final form of the equation are determined according to the following equation:

$$g(\lambda) = \int_{D_{min}}^{D_{max}} \frac{\pi}{4} D^2 \cdot Q_{ext}(D, \lambda, n) \cdot N(D). \quad (3)$$

Using $K_{j,i}$ to represent the part of the equation that takes into account the droplet dimensions and f_j to stand for the quantities concerning the number of the droplets, the above relation can be written as:

$$\begin{pmatrix} g(\lambda_1) \\ \vdots \\ g(\lambda_m) \end{pmatrix} = \begin{bmatrix} K_{1,1} & \cdots & K_{1,n} \\ \vdots & \ddots & \vdots \\ K_{m,1} & \cdots & K_{m,n} \end{bmatrix} \cdot \begin{pmatrix} f(D_1) \\ \vdots \\ f(D_n) \end{pmatrix}, \quad (4)$$

where $g(\lambda_i)$ is the vector determined during a direct measurement on the spectrometer, $K_{j,i}$ is the matrix calculated by means of the Mie procedures, and function f_j is a vector to be determined after a transformation from the above relation. In this case, a need arises to solve an inverse problem, where it is necessary to find the inverse matrix $K_{j,i}^{-1}$. In other words, the following equation has to be solved:

$$f_j = K_{j,i}^{-1} \cdot g_i. \quad (5)$$

The literature offers a few methods for the problem solving. The most common are the Philips method [34] and the Lawson–Hanson method [35], using the classic non-negative least squares (NNLS) approach. The NNLS method is a regression method that guarantees that only positive (or zero) coefficients are obtained. The method solves the above equation as:

$$\min_f \|K \cdot f - g\|^2, \text{ where } f \geq 0.$$

The real measuring system is composed of a few elements. The probe optical system, the task of which is to create the light space, is composed of a halogen–deuterium illuminator and optical fibers, connecting the illuminator to the probe head (collimator) and sending weakened light from the head to the spectrometer. In the SUT solution, the collimators placed in both probes (transmitting and receiving) are mounted on a traverse beyond the windowpanes, in the tunnel walls, thus not interfering with the flow through the nozzle and making it possible to reposition them easily during the testing. Figure 3 shows the two solutions for the probe mounting tested during these works: in the first, the probe is placed on a movable traverse, and in the second, it is permanently attached to the tunnel windowpanes. Considering the measurement characteristics, both solutions gave very similar results, so only the probe with collimators placed on the traverse was used for further analysis.

The calculation procedure presented earlier results in the determination of the number of droplets and their size. In most cases, the latter is reduced to the determination of the Sauter diameter according to the following formula:

$$D_{32} = \frac{\int_{D_{min}}^{D_{max}} D^3 N(D) dD}{\int_{D_{min}}^{D_{max}} D^2 N(D) dD}. \quad (6)$$

As is known, in the case of measurement techniques, it is important to be aware of the measurement uncertainty. In the case of LEM, it is usually up to 5% around the lower measurement range. Moving away from the lower measurement range, for small particles of the order of 0.1 μm , the measurement uncertainty decreases significantly. The applied LEM is used not only for the quantitative identification of water droplets resulting due to water vapor spontaneous condensation but also for the measurement of other liquid or solid particles [36]. The accuracy of this method requires validation for many of the data obtained for the reference samples.

2.4. Experimental Method

Apart from the atmospheric air pressure and temperature values, the important thing is the knowledge of the air relative humidity, i.e., the content of water vapor in the air, which is defined as:

$$\Phi_0 = \frac{p_v}{p_s(T_0)}, \quad (7)$$

where p_v is partial pressure of the air water vapor fraction, whereas p_s is the saturation pressure at ambient parameters—here, at the reference temperature.

Relative humidity of 0 means completely dry air, while 1 is air fully saturated with water vapor. A further increase in the water vapor content to values exceeding 1 (100%) results in vapor condensation.

In addition to relative humidity, another important aspect is the information on the wetness fraction, i.e., the mass of water vapor per unit of dry air mass. In the literature, this quantity is often marked as x :

$$x = \frac{m_v}{m_a} = \frac{p_v}{p_a} \cdot \frac{M_v}{M_a} = \frac{p_v}{p_0 - p_v} \cdot \frac{M_v}{M_a} = \frac{\Phi_0 \cdot p_s(T_0)}{p_0 - \Phi_0 \cdot p_s(T_0)} \cdot \frac{M_v}{M_a}. \quad (8)$$

It might seem that by measuring the temperature, pressure and relative humidity fully sufficient information will be obtained on the state and quality of the air. But, in the case of raw-air testing, it is also necessary to know the content of particulate matter in the atmospheric air, especially if the testing is carried out in urban centers. Such information can be obtained by measuring the level of the air pollution with particulate matter (solid particles/dust), e.g., PM1, PM2.5, PM4, PM10, where the number at the end denotes the diameter expressed in micrometers of the particle the content of which in the air is being measured. The particulate matter average density can be taken in the range of 1100–1300 kg/m^3 . Therefore, having the results of the pollution level measurement

expressed by the ratio of the mass of dust of a given diameter to the volume of air in which the particulates are contained, it is easy to estimate the boundary conditions at the inlet that are needed to model heterogeneous condensation. For a given PM measurement value for a given diameter D_{PM} , when knowing the air density and the adopted density of particulate matter D_{PM} , the number of particles per 1 kg of air can be calculated according to Equation (9).

$$\frac{PM \cdot 10^{-6}}{\rho_a} = \frac{1}{6} \pi D_{PM}^3 \rho_{PM} N_{PM}. \quad (9)$$

A number of measuring campaigns were carried out during the experimental research, in which selected physical phenomena were studied using the above-mentioned measuring techniques, including the following:

- Analysis of the process of spontaneous condensation of water vapor in flows through nozzles with different expansion rates for raw parameters of moist air. The aim was to establish the impact of the nozzle expansion rate on the intensity and location of the process of the liquid-phase formation.
- Measurement using a particulate filter for the selected nozzle geometry. Analysis of the impact of particulates contained in the air on the condensation process; in particular, on heterogeneous condensation.
- Measurement of selected nozzles with air heating at the test section inlet. The aim of the measurement was to perform testing for a relative humidity value lower than ambient. Assuming a constant moisture content in the air (constant water vapor mass fraction), determined for ambient conditions, the relative humidity value was recalculated for a higher value of temperature using Formula (8).
- For selected conditions and geometries, measurements were carried out of the impact of the size and number of droplets for constant relative humidity at a temperature rise at the test section inlet. The relative humidity value was kept constant by increasing the water vapor mass fraction in the air.

3. Results and Discussion

As already mentioned in the previous section, a limitation of the test rig used to investigate the phenomenon of water vapor condensation in the transonic flow of moist atmospheric air was the backpressure value of about 52 kPa at the nozzle outlet. For this reason, there is a supersonic to subsonic flow transition at the nozzle outlet in the form of a normal wave and oblique shock waves.

3.1. Effect of the Nozzle Expansion Rate on the Process of Water Vapor Spontaneous Condensation

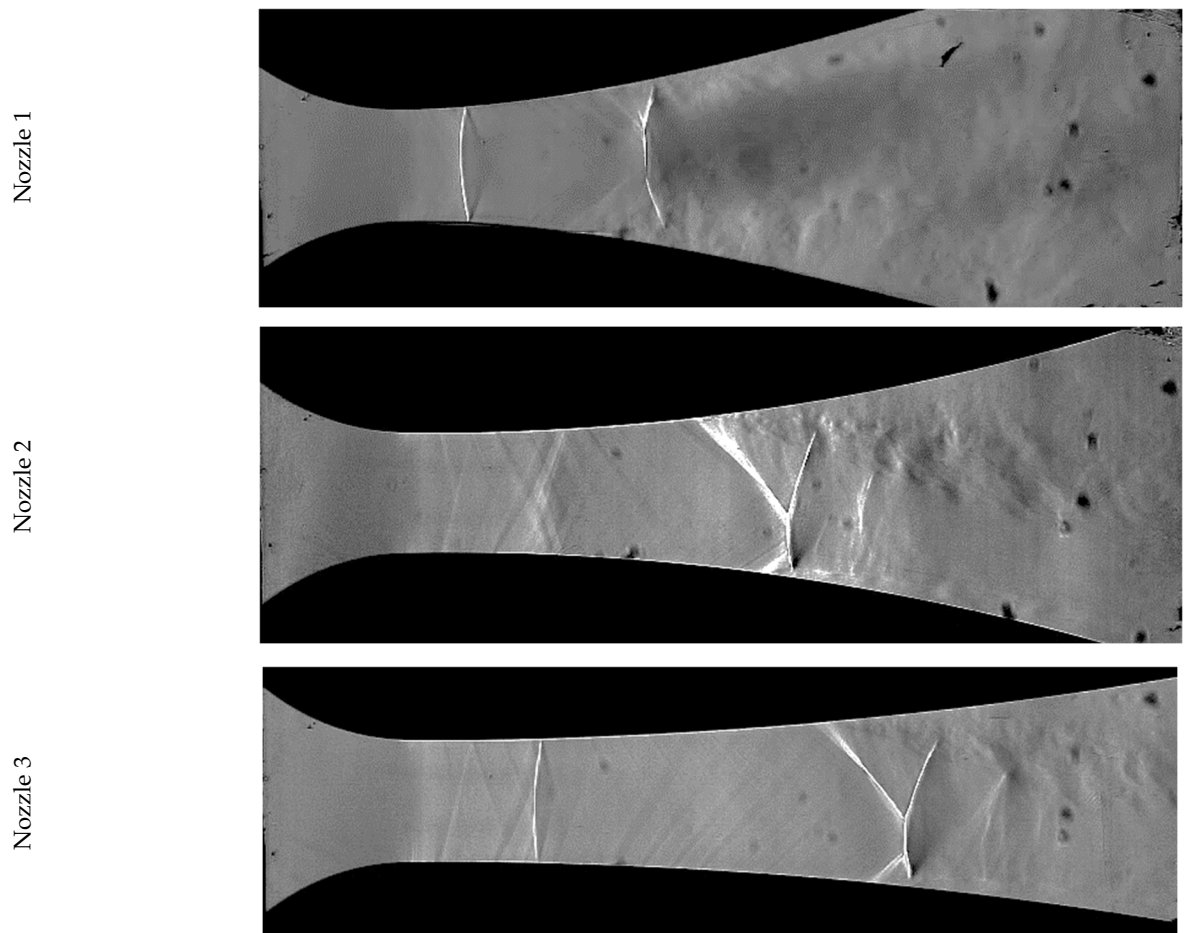
Three nozzle geometries with different degrees of opening in the divergent part were adopted for the tests to ensure different expansion rates following the data in Table 1. Table 2 shows the boundary conditions during the measurements in the three analyzed nozzles, which include thermodynamic data at the inlet and air quality parameters in the form of PM. As can be seen, only in the case of the measurements for Nozzle 2 was the level of air pollution elevated, but it still did not disturb the spontaneous condensation process.

Table 2. Boundary conditions for the analyzed cases of flow through the nozzles.

	Nozzle 1	Nozzle 2	Nozzle 3
p_0 , kPa	100.2	99.22	97.16
t_0 , °C	12	9.1	8.9
Φ_0 , %	91	86.5	83.7
PM1.0, µg/m ³	7	40	9
PM2.5, µg/m ³	7	48	10
PM4.0, µg/m ³	7	53	10
PM10, µg/m ³	7	55	10

Table 3 presents images obtained using the Schlieren technique for three nozzle geometries. In these photographs, at the exit of the nozzles, the shock wave structure in the form of a compound of normal and lambda waves is visible, which is a representation of the transition from supersonic to subsonic flow conditions. Since the backpressure value was the same for all cases (52 kPa) the position of these wave structures depends on the expansion rate. As the expansion rate increases, the transition from the supersonic to subsonic flow is closer to the nozzle's throat.

Table 3. Schlieren photographs for the analyzed cases.



The condensation wave is visible just behind the critical section of the nozzle (nozzle's throat). The position and intensity of the condensation wave depend, of course, on the nozzle geometry, mainly the expansion rate but also the boundary conditions at the inlet. In the case of Nozzles 1 and 3, the condensation process is very rapid, which is illustrated by a very clear condensation wave, while for Nozzle 2, spontaneous condensation occurs less rapidly and the condensation wave takes the shape of the letter "X".

The comments presented above are also reflected in the static pressure distribution on the upper wall of the nozzle shown in Figure 5.

Table 4 contains quantitative information on the liquid phase formed as a result of spontaneous condensation for all three cases analyzed here.

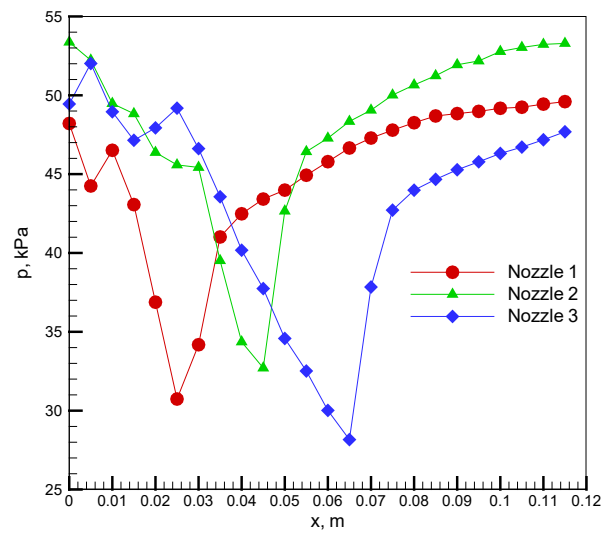
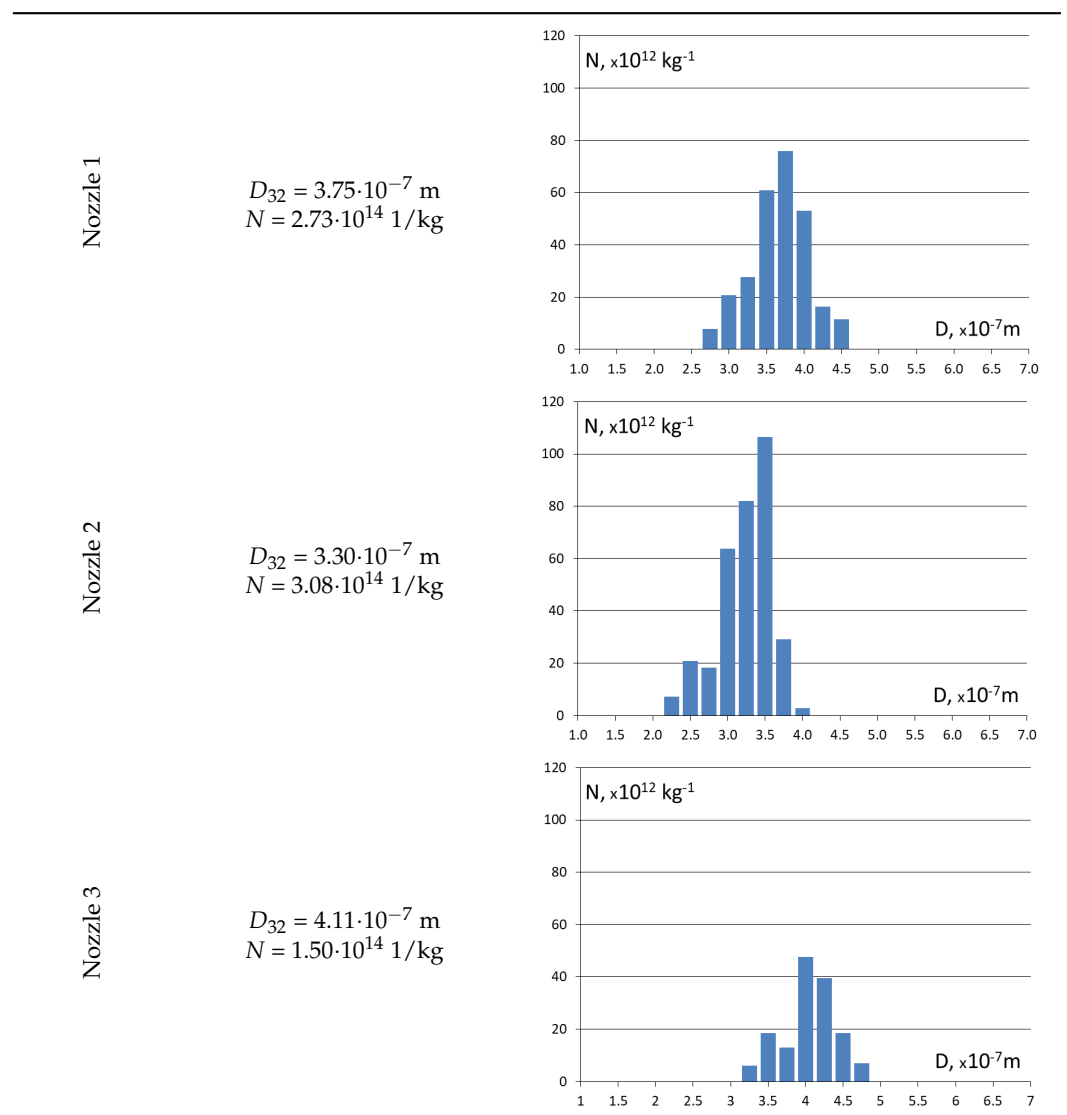


Figure 5. Static pressure distributions on the top wall of the investigated nozzles.

Table 4. Sauter diameter and droplet size distribution in the nozzle center line at a distance of 40 mm from the critical section.



The LEM measurement was performed in the center of the nozzle at a distance of 40 mm from the critical cross-section. This position guaranteed a measurement downstream of the condensation wave for all three cases but upstream of the normal wave. The table contains information about the mean Sauter diameter, the number of droplets in a kilogram of air, and the distribution $N = f(D)$. It is visible that the intensity of the steam condensation process increases the size and number of the liquid droplets.

3.2. Impact of Particulates on the Process of Water Vapor Spontaneous Condensation in the Nozzle

In all the cases under analysis, in addition to the thermodynamic parameters, the amount of particulate matter contained in the atmospheric air at the time of the measurement was measured at the nozzle inlet. The measurements were performed in the center of a city with a population of 200,000 people. Naturally, the presence and the level of PM air pollution depend on the atmospheric conditions and on the time of day and year. In the case of Nozzle 2, the values of the airborne particulate matter in one of the measurements had the highest values (Table 5). For this case, the measurements were performed with (Figure 6) and without a filter. The applied channel filter removes over 90% of particulates and guarantees a minimal drop in pressure at the level of about 200 kPa.

Table 5. Boundary conditions for the measurement, taking into account the effect of the presence of particulate matter in the air on the water vapor condensation process.

	Nozzle 2
p_0 , kPa	98.76
t_0 , °C	9.6
Φ_0 , %	71.3
PM1.0, $\mu\text{g}/\text{m}^3$	69
PM2.5, $\mu\text{g}/\text{m}^3$	72
PM4.0, $\mu\text{g}/\text{m}^3$	72
PM10, $\mu\text{g}/\text{m}^3$	72

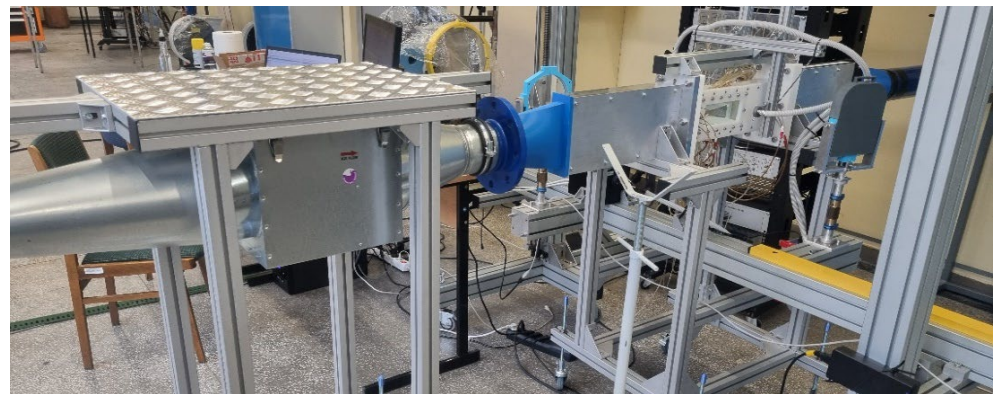


Figure 6. Air filter mounted in the test rig measuring system.

As an approximation, it can be assumed that this is a case of airborne particulate matter with an average density of mainly $1200 \text{ kg}/\text{m}^3$. Assuming that most particles have diameters of $1 \mu\text{m}$, Formula (9) can be used to calculate the number of dust particles, which in this case will total about $1 \cdot 10^{11}$ particles per kg of air.

The measurements performed with and without a filter showed no differences in the flow field visualization, but some small differences were observed in the distribution of the static pressure measured on the nozzle's top wall (Figure 7).

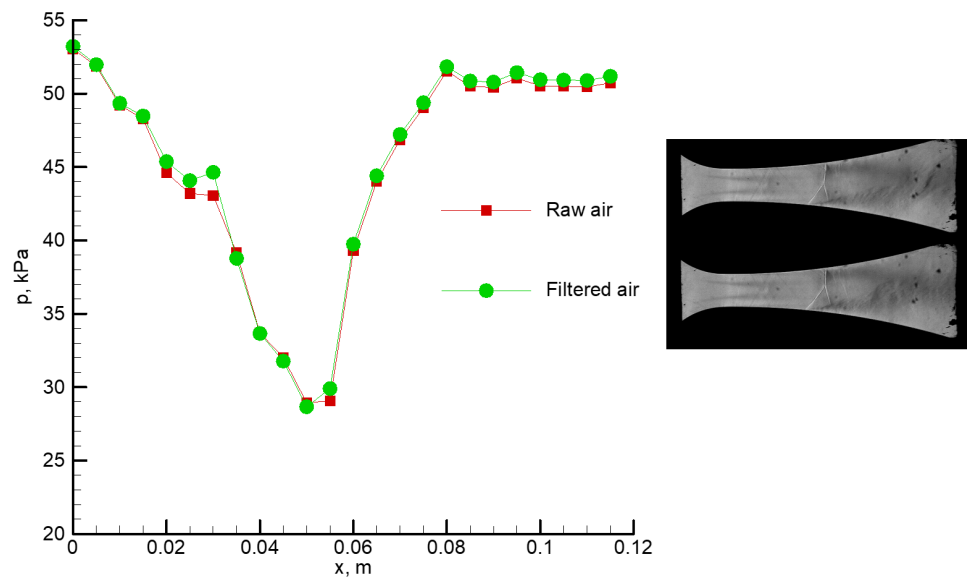


Figure 7. Comparison between the static pressure distributions on the Nozzle 2 top wall for the flow of raw and filtered air.

In the case of the filtered air flow, there is a slightly more intense condensation wave, located minimally closer to the critical section. These differences, however, are very small, which indicates that at this level of air pollution, the impact on the condensation process is slight. Similarly, it should not affect the size and number of the liquid droplets created due to the condensation process either.

3.3. Impact of the Relative Humidity Value on the Process of Water Vapor Spontaneous Condensation in the Nozzle

It is obvious that it is impossible to influence the parameters of the atmospheric air, humidity in particular. An extreme possibility for changing the air humidity in research test systems intended for the analysis of internal flows of air, for example, in nozzles, is to dry the inlet air. Another possibility resulting in a change in humidity is to heat the air a bit. The water vapor mass fraction then remains the same, but the water vapor saturation pressure is changed, which involves a change in relative humidity. In the presented research, the inlet air temperature was raised using a flow air heater (Figure 8).



Figure 8. Flow air heater with the test system.

Using Formulae (7) and (8), it is easy to calculate the change in the air relative humidity from the initial state to the state after the air temperature was raised. The inlet parameters for the reference state are as follows: total pressure: 97.16 kPa, total temperature: 8.9 °C, relative humidity: 83.7%. An increase in the inlet air temperature to 20 °C involves a

change in the relative humidity, whose value will total 43% in this case. A further increase in temperature by 10 degrees to the value of 30 °C results in a drop in relative humidity to 24%.

Table 6 presents the Schlieren photographs for the three cases under analysis for Nozzle 3. In the reference case, with no change in temperature, the condensation wave can be seen clearly right downstream of the nozzle’s critical section. If the air relative humidity is decreased by a rise in the air temperature, the strong condensation wave transforms into mild condensation with a slight increment in pressure. This can be seen better in the static pressure distribution on the nozzle’s top wall, as presented in Figure 9.

Table 6. Schlieren photographs for Nozzle 3 with different values of inlet temperature.

$t_0 = 30\text{ }^\circ\text{C}$, $\phi_0 = 24.7\%$ $t_0 = 20\text{ }^\circ\text{C}$, $\phi_0 = 43.7\%$ $t_0 = 8.9\text{ }^\circ\text{C}$, $\phi_0 = 83.7\%$

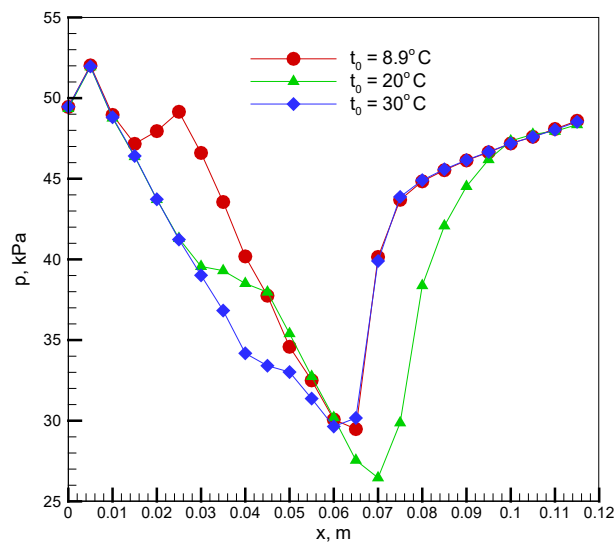
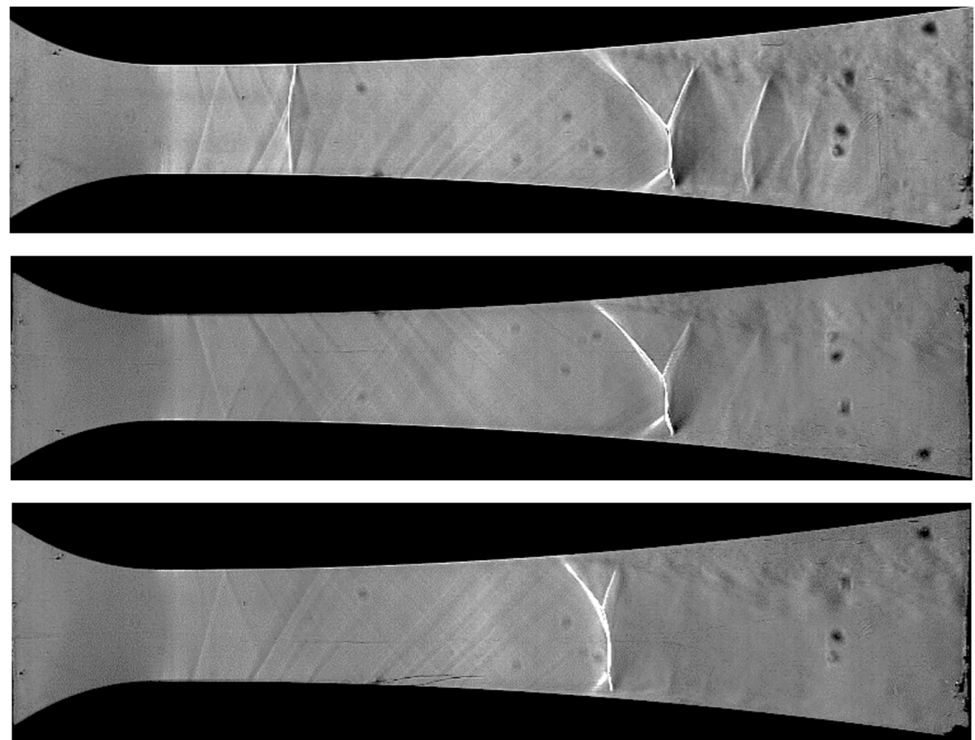
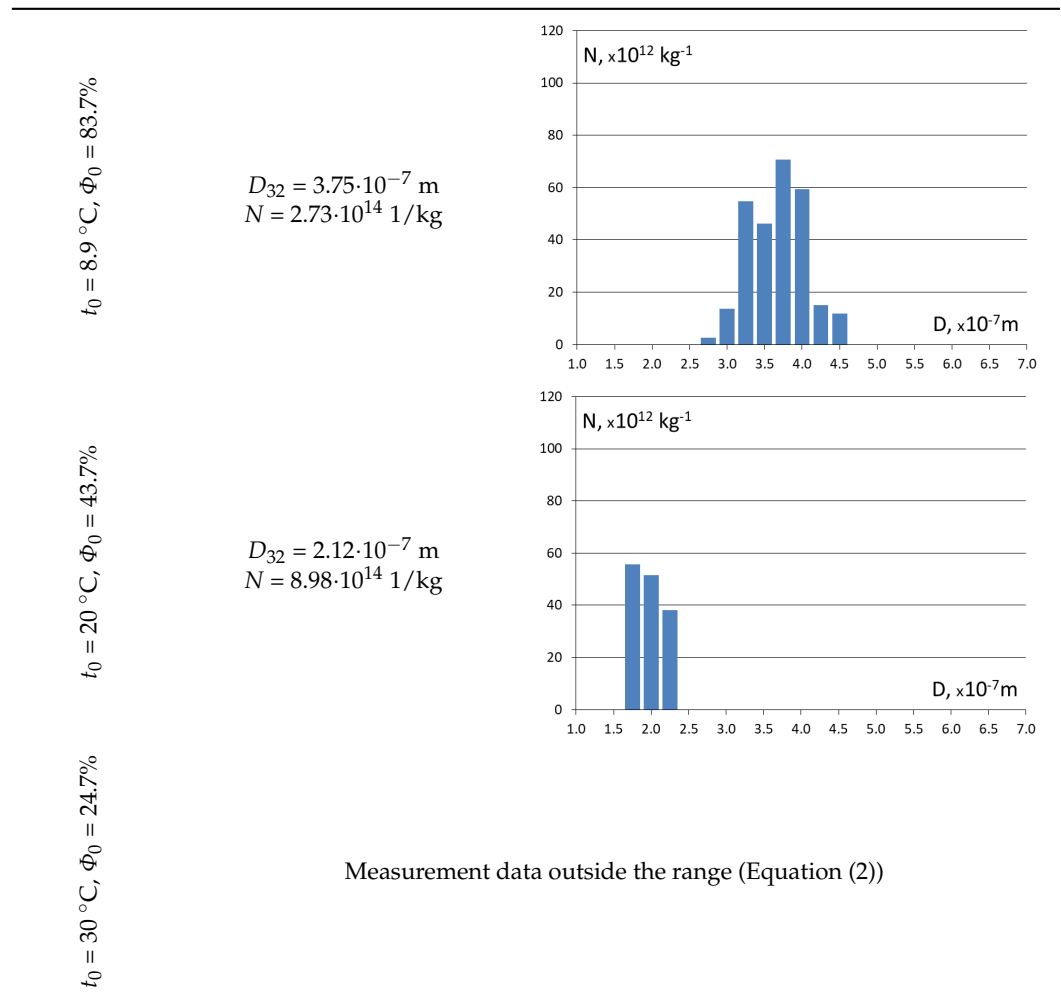


Figure 9. Static pressure distributions on the top wall of Nozzle 2 for different inlet temperature and relative humidity.

The weakening of the condensation process’s intensity is also accompanied by a decrease in the amount of condensed water vapor at a distance of 40 mm from the nozzle’s throat (Table 7). If the temperature is raised to 30 °C, the relative humidity value at the inlet is so low that very tiny droplets are formed only due to spontaneous condensation, below the measurement range of the LEM.

Table 7. Sauter diameter and droplet size distribution in the nozzle center line at a distance of 40 mm from the critical section for Nozzle 3 at variable relative humidity at the inlet.



3.4. Impact of a Change in the Air Temperature at a Constant Relative Humidity Value on the Process of Water Vapor Spontaneous Condensation in the Nozzle

The last but not least important issue related to the condensation of water vapor contained in moist air is the study of the effect of the air temperature at a constant value of relative humidity. According to Relation (8), an increase in the air temperature at a constant relative humidity value requires an increase in the moisture content, i.e., in the water vapor mass fraction in the air. The tests for Nozzle 3 were carried out by selecting atmospheric conditions corresponding to a low temperature and high humidity to make the temperature impact as visible as possible (Table 8).

The initial content of moisture at ambient parameters was 0.0032 kg of water vapor per 1 kg of air. If the temperature was raised by 10 degrees, the moisture content value had to be raised almost twice to 0.0061. An increase in temperature to 40 °C, keeping a similar relative humidity value of the air, required an almost tenfold rise in the moisture content, to 0.0387 of water vapor per 1 kg of air. At a known value of the critical mass flow through the tested nozzle, an appropriate amount of water vapor was injected at the nozzle inlet to

maintain a constant value of relative humidity. Figure 10 shows the relationship between the size of the droplets and their number when the temperature increases while keeping a constant value of relative humidity. It can be concluded that a significant increase in the mass of the liquid phase resulting from condensation with an increase in the temperature is mainly achieved by increasing the size of the drops while reducing their number.

Table 8. Boundary conditions for the reference case and for two cases with an increased value of the inlet air temperature.

	Nozzle 2
p_0 , kPa	96.50
t_0 , °C	0.8, 20, 30
Φ_0 , %	76.7
PM1.0, $\mu\text{g}/\text{m}^3$	45
PM2.5, $\mu\text{g}/\text{m}^3$	50
PM4.0, $\mu\text{g}/\text{m}^3$	51
PM10, $\mu\text{g}/\text{m}^3$	52

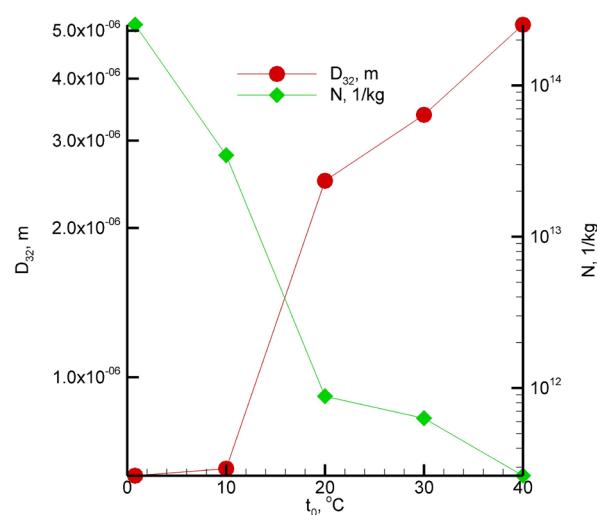


Figure 10. Temperature-dependent distribution of the mean diameter of the droplets and of the number of droplets at the air constant relative humidity.

4. Summary and Conclusions

It is difficult to find new experimental results concerning the phenomenon of non-equilibrium steam condensation due to the rapid expansion (cooling) of atmospheric air, both in external and internal flows. On the other hand, a lot of the literature that is available concerns the process of steam equilibrium condensation in air flowing at a low speed around heat exchanger surfaces. In light of this, the results of the experimental studies proposed in this paper fill the research gap and constitute a valuable material for the validation of numerical models for the non-equilibrium condensation of steam.

The presented complementary results of the experimental testing of the transonic flow of moist air in de Laval nozzles relate to the measurement of the pressure at the nozzle's top wall, the visualization of pressure waves in the nozzle by means of the Schlieren method, and quantitative measurements performed at selected points of the liquid phase (size and number of liquid droplets) formed due to the spontaneous condensation of water vapor contained in the air. In addition to this, information is provided on the boundary conditions, as well as on the geometry of the analyzed nozzles. Such a set of experimental data will enable reliable verification of the developed condensation models or CFD methods intended for the modeling of this kind of flow. It is known to those involved in the numerical modeling of two-phase flows with spontaneous condensation

that by manipulating the nucleation process and the droplet growth model, it is possible to approach the correct location and intensity of the condensation wave. With additional information on the number and size of the liquid-phase droplets, the process of adjusting the condensation model is more complete.

The aim of the presented research works was to provide experimental data verifying:

- the impact of the expansion rate in the nozzle on the location of the condensation wave formation and on the droplet size,
- the impact of the air relative humidity on the condensation conditions in the nozzle,
- the impact of the content of particulate matter in the air,
- the impact of a change in the inlet air temperature on the condensation process at constant relative humidity.

The results obtained from the measurements allow the following conclusions to be drawn:

- An increase in the nozzle expansion rate contributes to a faster occurrence of the processes of steam spontaneous condensation.
- An increase in the air relative humidity at the nozzle inlet causes a rise in the pressure increment on the condensation wave and in the amount of the formed liquid phase.
- Typical atmospheric air pollutants weaken the spontaneous condensation process very slightly.
- An increase in the air temperature while maintaining a constant level of relative humidity results in a decrease in the size of the droplets and a significant increase in their number.

It is shown that measurements of the size and of the number of water droplets formed due to the spontaneous condensation of moist air are possible using the light extinction method (LEM). However, it has to be emphasized that in the case of low contents of moisture, the measurement is close to the lower limit of the method's applicability, i.e., droplet diameters of about 0.1 μm .

The information on the number and size of the droplets formed due to rapid condensation obtained by means of the light extinction method (LEM) is a contribution to the development of research on the phenomena of the condensation of water vapor contained in moist air in transonic flows. Quantitative and qualitative measurements of the liquid phase, absent until now from the literature on moist air, are necessary to develop better numerical models, making it possible to correctly predict not only the condensation location but also the amount of the condensate.

Further research will focus on improving the experimental methods intended for quantitative identification of the dispersed phase in transonic flows of atmospheric air with a higher content of water vapor.

Author Contributions: Conceptualization, S.D., T.W., A.K. and F.T.; methodology, M.M. and S.D.; software, M.M.; validation, S.D. and T.W.; formal analysis, M.M. and S.D.; investigation, M.M., S.D. and K.S.; resources, M.M., S.D. and K.S.; data curation, M.M.; writing—original draft preparation, M.M., S.D. and K.S.; writing—review and editing, M.M., S.D., K.S., T.W., A.K. and F.T.; visualization, M.M. and K.S.; supervision, S.D., T.W., A.K. and F.T.; project administration, S.D. and T.W. All authors have read and agreed to the published version of the manuscript.

Funding: This work was performed within the research funded by Airbus Operations and by statutory research funds of the Silesian University of Technology.

Data Availability Statement: The original contributions presented in the study are included in the article, further inquiries can be directed to the corresponding author.

Conflicts of Interest: T.W. and A.K. were employed by Airbus Operations GmbH. F.T. was employed by Airbus Operations SAS. The remaining authors declare that the research was conducted in the absence of any commercial or financial relationships that could be construed as a potential conflict of interest. The authors declare that this study received funding from Airbus Operations. The funder

was not involved in the study design, collection, analysis, interpretation of data, the writing of this article or the decision to submit it for publication.

Nomenclature

c	speed of sound: m/s
D	diameter, m
I	light intensity, W/m ²
l	length, m
M	molecular mass, g/mol
N	number of particles, 1/kg
n	refractive index, -
p	absolute pressure, Pa
\dot{p}	expansion rate, 1/s
PM	particulate matter, µg/m ³
T	temperature, K
x	humidity ratio, -
X	Mie parameter, -
Greek symbols	
λ	wavelength, m
Φ	relative humidity, -
ρ	density, kg/m ³
Subscripts	
0	total conditions or the reference state
a	dry air
v	vapor
s	saturation

References

- Prandtl, L. Allgemeineüberlegungen die strömung zusammendrückbarer flüssigkeiten. In *Atti del V Convegno Volta*, 1st ed.; Roma Reale Accademia: Rome, Italy, 1936; Volume XIV, p. 167.
- Hermann, R. *Luftfahrt-Forschung*; XIX, 201; Mittler & Sohn Verlag: Hamburg, Germany, 1942.
- Oswatitsch, K. Kondensationserscheinungen in Überschalldüsen. *ZAMM J. Appl. Math. Mech.* **1942**, *22*, 1–14. [[CrossRef](#)]
- Zierep, J.; Lin, S. Bestimmung des Kondensationsbeginns bei der Entspannung von feuehter. *Luft. Forsch. Ing. Wesen* **1967**, *88*, 169–172. [[CrossRef](#)]
- Frank, W. Stationäre Kondensationsprozesse in Überschalldüsen. *Forsch. Ing. Wesen* **1983**, *49*, 189–194. [[CrossRef](#)]
- Schnerr, G.H. Homogene Kondensation in Stationären Transsonischen Strömungen Durch Lavaldüsen und um Profile. Ph.D. Thesis, Fakultät für Maschinenbau, Universität Karlsruhe, Karlsruhe, Germany, 1986.
- Schnerr, G. 2-D transonic flow with energy supply by homogeneous condensation: Onset condition and 2-D structure of steady Laval nozzle flow. *Exp. Fluids* **1988**, *7*, 145–156. [[CrossRef](#)]
- Bartlmä, F. Berechnung des Strömungsvorgangs bei Überschreiten der kritischen Wärmezufuhr. *DVL Ber.* **1961**, 168.
- Griffin, J.L.; Sherman, P.M. Computer Analysis of Condensation in Highly Expanded Flows. *AIAA J.* **1965**, *3*, 1813. [[CrossRef](#)]
- Puzyrewski, R.; Król, T. Numerical analysis of Hertz-Knudsen model of condensation upon small droplets in water vapor. *IFFM* **1976**, *70–72*, 285–307.
- Guha, A. A unified theory of aerodynamic and condensation shock waves in vapor-droplet flows with or without a carrier gas. *Phys. Fluids* **1994**, *6*, 1893–1913. [[CrossRef](#)]
- Setoguchi, T.; Matsuo, S.; Yu, S. Effect of Nonequilibrium Homogenous Condensation on Flow Fields in a Supersonic Nozzle. *J. Therm. Sci.* **1997**, *6*, 90–96. [[CrossRef](#)]
- Wiśniewski, P.; Dykas, S.; Majkut, M.; Smółka, K.; Nocoń, M.; Wittmann, T.; Friedrichs, J. A comprehensive analysis of the moist air transonic flow in a nozzle with a very low expansion rate. *Appl. Therm. Eng.* **2022**, *217*, 119185. [[CrossRef](#)]
- Wiśniewski, P.; Dykas, S.; Majkut, M.; Smółka, K. Analysis of the moist air transonic flow in the symmetric and asymmetric nozzle of the low expansion. *J. Phys. Conf. Ser.* **2022**, *2367*, 012031. [[CrossRef](#)]
- Schnerr, G.H.; Dohrmann, U. Transonic Flow Around Airfoils with Relaxation and Energy Supply by Homogeneous Condensation. *AIAA J.* **1990**, *28*, 1187–1193. [[CrossRef](#)]
- Schnerr, G.H.; Mundinger, G. Numerical Visualization of Self-Excited Shock Oscillations in Two-Phase Flows. In Proceedings of the 5th International Symposium on Computational Fluid Dynamics, Sendai, Japan, 31 August–3 September 1993; Daiguji, H., Ed.; Japan Society of CFD: Sendai, Japan, 1993.
- Schnerr, G.H.; Dohrmann, U. Drag and Lift in Nonadiabatic Transonic Flow. *AIAA J.* **1994**, *32*, 101–107. [[CrossRef](#)]
- Schnerr, G.H.; Heiler, M. Two-phase Flow Instabilities in Channels and Turbine Cascades. *Comput. Fluid Dyn. Rev.* **1998**, *II*, 668–690.

19. Zhang, G.; Yang, Y.; Chen, J.; Jin, Z.; Majkut, M.; Smolka, K.; Dykas, S. Effect of relative humidity on the nozzle performance in non-equilibrium condensing flows for improving the compressed air energy storage technology. *Energy* **2023**, *280*, 128240. [[CrossRef](#)]
20. Sokolichin, A.; Eigenberger, G.; Lapin, A.; Lübert, A. Dynamic numerical simulation of gas-liquid two-phase flows Euler/Euler versus Euler/Lagrange. *Chem. Eng. Sci.* **1997**, *52*, 611–626. [[CrossRef](#)]
21. Davy, G.; Reyssat, E.; Vincent, S.; Mimouni, S. Euler–Euler simulations of condensing two-phase flows in mini-channel: Combination of a sub-grid approach and an interface capturing approach. *Int. J. Multiph. Flow* **2022**, *149*, 103964. [[CrossRef](#)]
22. Ding, H.; Zhang, Y.; Yang, Y.; Wen, C. A modified Euler-Lagrange-Euler approach for modelling homogeneous and heterogeneous condensing droplets and films in supersonic flows. *Int. J. Heat Mass Transf.* **2023**, *200*, 123537. [[CrossRef](#)]
23. Wiśniewski, P.; Dykas, S.; Miyazawa, H.; Furusawa, T.; Yamamoto, S. Modified heat transfer correction function for modeling multiphase condensing flows in transonic regime. *Int. J. Heat Mass Transf.* **2023**, *201*, 123597. [[CrossRef](#)]
24. Marynowski, T.; Desevaux, P.; Mercadier, Y. CFD Modeling of the Two-Phase Flow in a Moist Air Powered Ejector. *J. Comput. Multiph. Flows* **2009**, *1*, 283–294. [[CrossRef](#)]
25. Zhang, G.; Yang, Y.; Chen, J.; Jin, Z.; Dykas, S. Numerical study of heterogeneous condensation in the de Laval nozzle to guide the compressor performance optimization in a compressed air energy storage system. *Appl. Energy* **2024**, *356*, 122361. [[CrossRef](#)]
26. Poškas, R.; Sirvydas, A.; Salem, M.; Poškas, P.; Jouhara, H. Experimental investigation of water vapor condensation from hot humidified air in serpentine heat exchanger. *Int. J. Heat Mass Transf.* **2024**, *221*, 125068. [[CrossRef](#)]
27. Yang, P.; Cao, X.; Liu, J.; Zhou, S. Experimental study of steam condensation heat transfer in an inclined tube at low mass fluxes. *Int. J. Heat Mass Transf.* **2024**, *224*, 125257. [[CrossRef](#)]
28. Siddiqui, M.; Azam, M.A.; Ali, H.M. Parametric Evaluation of Condensate Water Yield from Plain Finned Tube Heat Exchangers in Atmospheric Water Generation. *Arab. J. Sci. Eng.* **2022**, *47*, 16251–16271. [[CrossRef](#)]
29. Majkut, M. *Advanced Techniques of Experimental Research and Visualization of the Compressible Gas Flow in Power Engineering Machinery*; Silesian University of Technology: Gliwice, Poland, 2019. (In Polish)
30. Wang, Y.; Mu, X.; Shen, S.; Zhang, W. Heat transfer characteristics of steam condensation flow in vacuum horizontal tube. *Int. J. Heat Mass Transf.* **2017**, *108*, 128–135. [[CrossRef](#)]
31. Cai, X.S.; Wang, N.N.; Wei, J.M.; Zheng, G. Experimental investigation of the light extinction method for measuring aerosol size distributions. *J. Aerosol. Sci.* **1992**, *23*, 749–757. [[CrossRef](#)]
32. Cai, X.; Wanc, L.; Ouyang, X.; Pan, Y. A novel integrated probe system for measuring the two phase wet steam flow in steam turbine. *J. Eng. Thermophys.* **1992**, *22*, 52–57.
33. Majkut, M.; Dykas, S.; Smolka, K. Light extinction and ultrasound method in the identification of liquid mass fraction content in wet steam. *Arch. Thermodyn.* **2020**, *41*, 63–92. [[CrossRef](#)]
34. Twomney, S. On the Numerical Solution of Fredholm Integral Equations of the First Kind by the Inversion of the Linear System Produced by Quadrature. *J. ACM* **1963**, *10*, 97–101. [[CrossRef](#)]
35. Lawson, C.L.; Hanson, R.J. *Solving Least Squares Problems*; SIAM: Philadelphia, PA, USA, 1995.
36. Jiang, M.; Liu, X.; Han, J.; Wang, Z.; Xu, M. Influence of particle properties on measuring a low-particulate-mass concentration by light extinction method. *Fuel* **2021**, *286*, 119460. [[CrossRef](#)]

Disclaimer/Publisher’s Note: The statements, opinions and data contained in all publications are solely those of the individual author(s) and contributor(s) and not of MDPI and/or the editor(s). MDPI and/or the editor(s) disclaim responsibility for any injury to people or property resulting from any ideas, methods, instructions or products referred to in the content.